Real-Time Poling Vapor Co-deposition of Dye-Doped Second-Order Nonlinear Optical Polymer Thin Films

3 AUTHORS, INCLUDING:

Jwo-Huei Jou
National Tsing Hua University
158 PUBLICATIONS **2,064** CITATIONS

SEE PROFILE

Real-Time Poling Vapor Co-deposition of Dye-Doped Second-Order Nonlinear Optical Polymer Thin Films

Hua-Shu Wu, Jwo-Huei Jou,* and Yu-Chin Li

Department of Materials Science and Engineering, National Tsing-Hua University, Hsin-Chu, Taiwan 300, ROC

Jung Y. Huang

Institute of Electro-Optical Engineering, National Chiao-Tung University, Hsin-Chu, Taiwan 300, ROC

Received October 22, 1996; Revised Manuscript Received March 12, 1997[⊗]

ABSTRACT: Dye-doped second-order nonlinear optical (NLO) poly(amic acid) (PAA) and polyimide (PI) thin films were prepared via a newly developed real-time poling vapor co-deposition process. This method would plausibly enable many polymeric materials, including high glass transition ones, to be matrix films and many NLO-active chromophores to be desired dopants for making numerous NLO thin films. The PAA film, after curing at 150 °C, showed a considerable improvement in thermal stability. Fourier transform infrared characterization also revealed that a 23 wt % disperse red 1 doped PI thin film exhibited reasonable second harmonic generation (SHG) characteristics even at relatively low poling fields; that is, the SHG coefficient had increased from 0.8 to 5.8 pm/V for a poling field increasing from 0.01 to 0.1 MV/cm.

Introduction

Electrooptic applications of organic second-order nonlinear optical (NLO) materials have triggered tremendous research efforts in searching for the most applicable material synthesis and processing systems.[1−12] The primary requirement therein is to find the materials with sound NLO properties that would survive peak processing temperature while lasting for a sufficiently long time span in use. Though the peak processing temperature varies with different fabrications or may even decrease in future processes and the lifetime requirements are different for different end-use purposes, it is always desirable to have the NLO materials highly stable at elevated temperatures. If this is coupled with some other stringent requirements, not many systems or materials can possibly succeed.

The purpose of this study to present a new approach that would enable many polymeric materials, including high glass transition ones, to be feasible matrices and many NLO-active dyes to be the desired dopants for making numerous tailorable NLO thin films. This can be done by simultaneously co-depositing an NLO-active chromophore and polymer thin film forming monomer(s), while concurrently applying a poling field, electrically or otherwise. The current approach has indeed been proven successful via real-time poling vapor co-deposition in preparing a dye-doped poly(amic acid) thin film, which exhibited reasonable second harmonic generation characteristics. The film, after curing, further exhibited a considerable improvement in thermal stability. In the following sections, we will first show the corresponding theoretical calculation regarding the prospects of accomplishing a real-time poling process. Next we will reveal the experimental procedures and give detailed results and discussion concerning the NLO characteristics of the resultant thin films.

Theoretical Calculation

The poling time, t_p, required for a static NLO molecule at an angle θ with respect to the poling field (Figure 1)

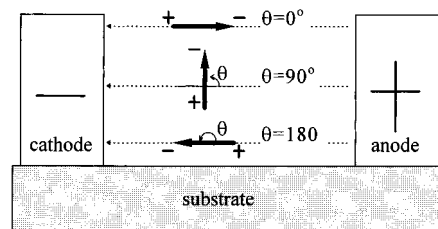**Figure 1.** Schematic diagram of NLO molecules at various angles with respect to the poling field in the poling zone.

has been derived as follows:[13]

$$t_p = \frac{\pi}{2}\sqrt{\frac{ma^2}{\mu E}}\Big\{1 + \Big(\frac{1}{2}\Big)^2 k^2 + \Big(\frac{1 \times 3}{2 \times 4}\Big)^2 k^4 + \Big(\frac{1 \times 3 \times 5}{2 \times 4 \times 6}\Big)^2 k^6 + ...\Big\} \quad (1)$$

where m, a, and μ, are the molecular mass, half of the charge separation distance, and the dipole moment of the NLO molecule, respectively. E is the poling field strength, where k is equal to $\sin(\theta/2)$. For example, the calculated poling time required to rotate an NLO molecule at 175°, with respect to the desired orientation, is from 1.9×10^{-10} to 6.1×10^{-11} s for a poling field ranging from 0.01 to 0.1 MV/cm.[14] Such a poling time should be sufficient to rotate more than 95% of the NLO molecules to the desired orientation, provided they are randomly oriented initially.

In practice, however, the evaporating NLO molecules are in a dynamic state. The time required for a 180° out of phase molecule to rotate to the desired poling direction is estimated to be 2.2×10^{-10}. This is even shorter than that required in the static state.

In order to real-time pole the NLO molecules, the poling time required for these molecules must not just be short; it has to be even shorter than its traveling time in the poling zone as well. Here, the traveling time is defined as the flight time of the dye molecule in the poling zone before it deposits onto the substrate. For calculation, the length of the poling zone is assumed to be equal to the thickness of the electrodes, which is 0.3
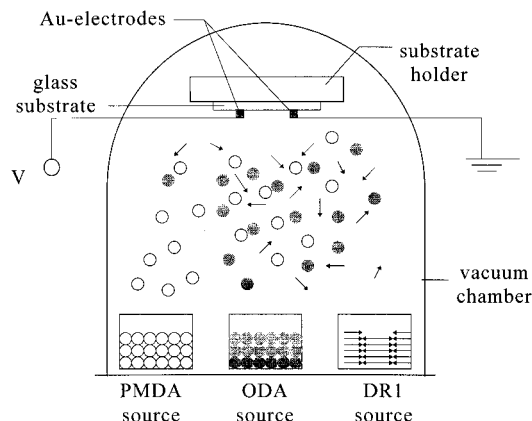
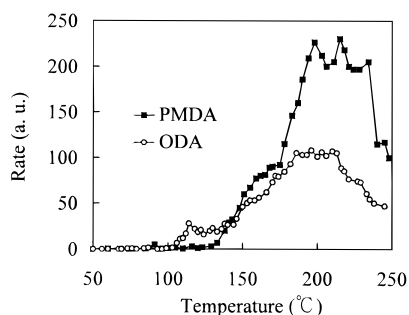**Figure 2.** Schematic diagram of the VDP system coupling with a real-time poling setup.

Figure 3. Deposition rates of PMDA and ODA monomers as a function of temperature.

μm. This distance will take the NLO molecules 1.7×10^{-9} s to travel before depositing on the substrate.[15] Since the poling time required is shorter than the traveling time in the current system, the NLO molecules can thus be expected to be real-time poled during the co-deposition process.

Experimental Section

Materials. The NLO dye molecule used was the disperse red 1 (DR1) and this was purchased from Alrich Chemical Co., Inc. The polymer thin film forming monomers were dianhydride, pyromellitic dianhydride (PMDA), which was purchased from Chrisken Company, Inc., and the diamine, 4,4′-diaminodiphenyl ether (ODA), which was purchased from Tokyo Kasei Kogyo Co., Ltd. These materials were used as received.

Vapor Deposition Polymerization. A schematic diagram of the vapor deposition polymerization (VDP) system coupled with a real-time poling setup is shown in Figure 2. The NLO polymer thin films were prepared by simultaneously co-depositing 0.025 g of DR1 molecules and 0.2 g each of the monomers on a glass substrate using thermal evaporation. The deposition process began in a vacuum of 5×10^{-5} mbar.

To better control the stoichiometric ratio of the two monomers, the temperature-dependent deposition rates of the two monomers and DR1 were separately determined by using a Maxtek TM-200R quartz oscillation thickness monitor prior to the co-deposition process.

Poling. For poling, the glass substrate used was first prepatterned with pairs of gold (Au) electrodes, which were 0.3 μm thick with spacings of 100, 200, 500, and 1000 μm, respectively. An electrical voltage of 1500 V was applied through the paired electrodes concurrently during the deposition process.

Curing. Thermal curing of some of the as-deposited samples was carried out in a vacuum after the deposition process. The specimens were elevated to 150 °C at a ramp rate of 3 °C/min and held for 30 min. The same poling field was applied throughout the curing process until it had cooled down to below 40 °C.

FTIR Characterization. The structure and composition of the resultant films were characterized using Fourier transform infrared (FTIR) spectrometry. The FTIR experiment was done by using a Bomem DA 3002 spectrometer. The machine resolution was 2 cm^{-1}. The spectra with wavenumbers ranging from 500 to 2000 cm^{-1} were recorded.

SHG Measurement. Second harmonic generation (SHG) of the resultant specimens was measured to investigate the effectiveness of the poling process. The SHG measurement was performed using a Q-switch Nd:Yag laser ($\lambda = 1064$ nm) with a Y-cut quartz crystal reference ($d_{11} = 0.5$ pm/V). The incident laser beam, with a power of 2.7 mW, was targeted at the spacing between the electrodes, and the SHG signal (532 nm) was measured after it had passed through the sample.

Results and Discussion

Figure 3 shows the deposition rates of the PMDA and ODA monomers as a function of evaporation temperature. The PMDA monomer began to evaporate markedly at 120 °C at 5×10^{-5} mbar. Its deposition rate increased as the temperature increased until it reached a maximum reading at 190 °C. Similarly, the ODA monomer also evaporated markedly, but only at 90 °C, and had a maximum deposition rate at 175 °C. Declination of the deposition rates, after reaching the maxima, resulted from the depletion of the monomer sources added.

To achieve a high degree of polymerization, it was required to accurately control the stoichiometric ratio of the PMDA and ODA monomers. In Iijima's study,[16] deposition of the monomers had been fixed at constant temperatures, e.g. 180 °C for PMDA and 160 °C for ODA. In this study, the stoichiometric ratio of the deposition monomers was controlled by separately controlling the ramp rates of the two different monmer sources. Before the beginning of the deposition process, the source boats were preheated to 10 °C below the starting deposition temperatures. This procedure allowed the source boats to be ramped up smoothly. Reasonably good films had been obtained by co-depositing the PMDA monomer from 120 to 160 °C with a ramp rate of 4 °C/min and the ODA monomer from 90 to 140 °C with a ramp rate of 5 °C/min. The molar ratio of ODA to PMDA was found to be 1.2 at the beginning of the deposition process, and 0.7 at the end. The average molar ratio of ODA to PMDA in the resultant thin films was estimated to be 1.1. The resultant thin films were 0.7 ± 0.1 μm thick.

Doping via Co-deposition. Deposition condition of the NLO-active DR1 was characterized in the same manner. The evaporation rate markedly rose at 120 °C and reached a maximum rate at 150 °C. In order to dope the DR1 molecules into the aforementioned polymer thin film, the DR1 molecules were co-deposited simultaneously during the deposition of the two polymer-forming monomers. Deposition of the DR1 molecules was started at 120 °C and stopped at 160 °C over 4 min. The as-deposited films were red and transparent, uniformly covering the entire substrate. The film color did not change upon annealing at 150 °C for 30 min. This annealing process allowed the as-deposited films to transfer, at least partly, from poly(amic acid) to polyimide.

FTIR Results. Figure 4 shows the FTIR spectra of the films before and after curing. For the as-deposited film, an absorption peak at 1650 cm^{-1} was observed, which corresponded to the characteristic absorption of the amide carbonyl group of PAA.[16] This confirms the formation of the PAA structure. However, absorption peaks corresponding to the pure PMDA monomer were
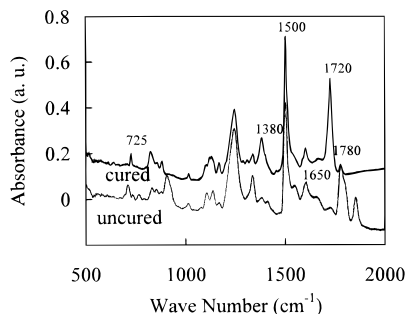
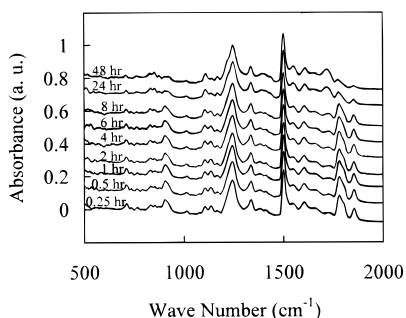**Figure 4.** FTIR spectra of the DR1 doped PMDA-ODA film before and after curing.

Figure 5. FTIR spectra of the as-deposited film at varying storage times. The film was purposely stored in air.
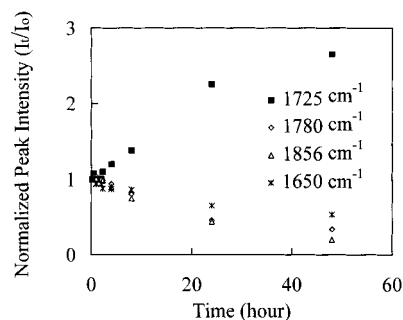

Figure 6. Variations of the characteristic FTIR peak intensity with respect to time of the as-deposited film.

also observed at 1780 and 1850 cm^{-1}.[17] The as-deposited films seemed to possess some unreacted monomers.

After curing, the imide absorption peaking at 725, 1380, 1720, and 1780 cm^{-1} clearly appeared, indicating that the PAA structure had been converted into the PI counterpart.[16] In contrast, the absorption peaks of the unreacted PMDA monomer disappeared altogether. The residual unreacted monomers may have further reacted or sublimated during the curing process. The peak of the amide at 1650 cm^{-1}, however, did not diminish completely, suggesting that some of the PAA chains had not been converted. Higher curing temperatures might have improved the extent of imidization. However, any elevation of the curing temperature should be carefully performed so that the DR1 molecule would not sublimate or degrade thermally.

Degradation of the as-deposited films was observed when they were stored in air. Figure 5 shows the change in FTIR spectra of an as-deposited film with storage time increasing from 0.25 to 48 h. As storage time increased, the characteristic absorption peaks of the dianhydride monomer at 1780 and 1850 cm^{-1} and that of the amide at 1650 cm^{-1} decreased, while that of the carboxylic acid at 1725 cm^{-1} increased. Figure 6 shows with respect to time the variations of the corre-
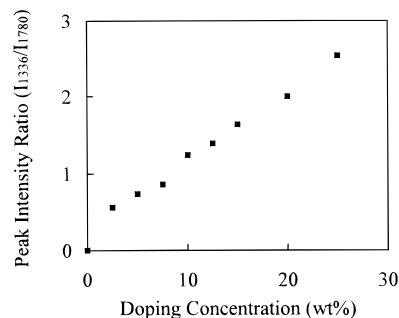

Figure 7. Correlation curve of the FTIR peak intensity ratios of DR1 to the internal standard with the weight fractions of DR1 in the DR1 mixed PAA films.

sponding peak intensities. The decrement of the amide and dianhydride peak intensities indicates the diminishment of the unreacted PMDA monomer and previously formed PAA in the films. Both the dianhydride and amide are believed to hydrolyze to their carboxylic acid counterparts. This can be supported by the change in the carboxylic acid intensity as seen in the same figure. Hence, hydrolysis can be concluded to be the major cause of the degradation of the as-deposited films stored in air.

Composition Result. Compositions of the resultant films can be determined by knowing the deposition rates of the three molecules. This, however, requires three sets of thickness monitors, which were not available in the system. The composition was hence determined by establishing a composition curve correlating the DR1 weight fraction with its absorption peak intensity from FTIR.

This was done by preparing a series of DR1 mixed PAA films with known compositions. The PAAs used for this purpose were obtained using the conventional synthesis method. The films, after curing at 150 °C for 30 min, were characterized using FTIR. One major characteristic absorption peak of DR1 appeared at 1336 cm^{-1}, which corresponded to the absorption of its nitro group.[18] This peak was hence used to correlate the weight fraction of the DR1 molecules in the resultant VDP films. To eliminate the effect of film thickness variation, the obtained peak intensity of DR1 was divided by that of an internal standard. The internal standard chosen was the peak at 1780 cm^{-1}, which corresponded to the absorption of the imide group.

Figure 7 shows the peak intensity ratios of 1336 cm^{-1} (of DR1) to 1780 cm^{-1} (of PI) with various different DR1 doping fractions. The ratio increases linearly with the increase of the DR1 concentration ranging from 2.5 to 25 wt %. According to this correlation curve, the DR1 in the resultant VDP thin films was determined to be 23 wt %.

Poling Effectiveness. Figure 8 shows the effect of poling field strength on the SHG coefficient of the resultant thin films. All the poled regions of the thin films yielded a SHG signal, regardless of the strength of the poling field. It is noteworthy that the film yielded a marked SHG signal even at a relatively low poling field of 0.01 MV/cm. For the films that were only poled after deposition, no SHG signal was detected after the same curing procedure. This validates the feasibility of real-time poling of the current system. The SHG coefficients increased with the increase of the poling field strength, indicating that thermal fluctuation of the NLO active molecules can be better restrained in the presence of a stronger poling field.
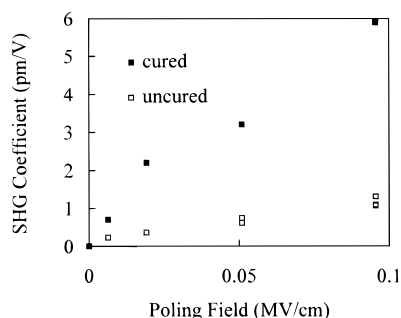
Figure 8. SHG coefficient d_{33} as a function of poling field for the resultant thin films, where the subscript 3 denotes the direction along the poling field.
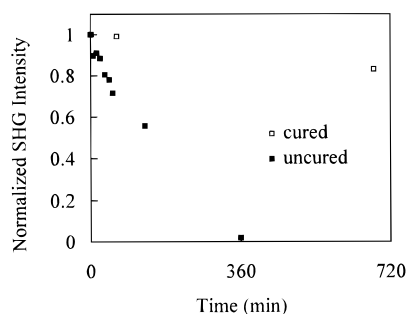

Figure 9. Variation of the SHG intensity with respect to time of the resultant thin films at room temperature.

The SHG intensities of the uncured samples were comparatively smaller than those of the cured ones. This may be due to the fact that the uncured PAA films can easily be attacked by moisture as revealed previously. Before each SHG measurement, about 40 min was taken to load the samples. During this period, the samples were exposed to air, and the film integrity of the uncured films was somewhat degraded. As a result, some of the preoriented dye molecules could no longer be constrained and so the corresponding SHG intensity dropped.

Figure 9 shows with respect to time the variation of the SHG intensity for the resultant thin films at room temperature. For the uncured one, the SHG intensity rapidly decreased with time and vanished after 6 h. This should be attributed to the moisture-attack-induced degradation of the PAA polymer matrix as mentioned above. Contrarily, the cured one exhibited much better stability. Its SHG intensity remained at 88% of its original intensity after 12 h. The curing process did improve the film stability, though the film was not fully imidized.

Curing Effect. The temporal stability of the films was also investigated at some other temperatures. The results are shown in Figures 10 and 11 for the uncured and cured films, respectively. In both cases, every obtained intensity was normalized to the intensity measured at room temperature. When the uncured samples were exposed to elevated temperatures, the SHG signals underwent a rapid decay initially and then gradually leveled off after a certain time period. The decay was more marked at higher temperatures. At 140 °C, the signal decayed to zero within 50 s. The polymer matrix could no longer constrain the randomly occurring reorientation movement of the DR1 molecules at this elevated temperature.

Although the cured films exhibited a similar relaxation behavior, the initial decay was much less marked. For example, the intensity of the cured film dropped by
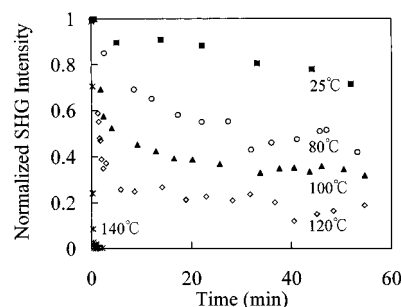

Figure 10. SHG relaxation of the uncured films at different temperatures.
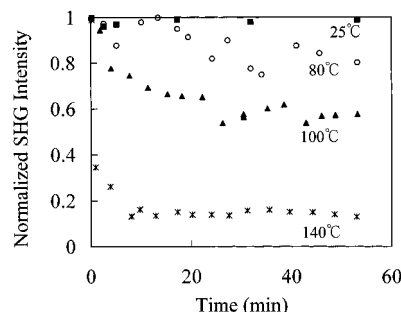

Figure 11. SHG relaxation of the cured films at different temperatures.

40% in 20 min at 100 °C, while for the uncured one it dropped by 60%. At 140 °C, the intensity of the cured film retained 16% of its initial value for more than 40 min with no further decay indication. The thermal stability of the thin films was greatly improved by the curing process. As pointed out by Wu et al., the films cured at higher temperatures exhibited a higher thermal stability in their SHG characteristics.[19] Some of the specimens were further cured at higher temperatures. The curing, with the presence of a poling field, was successful at 180 °C, but failed at 200 °C, due probably to the decomposition of the dye. Since the curing process has been proven to be a success in improving the stability, it is highly plausible that similar NLO thin films could be stable at higher temperatures if higher curing temperatures were employed. This would then demand a more thermally stable NLO-active chromophore.

Conclusion

Nonlinear optical polymer thin films of the guest−host type have been successfully prepared by using vapor co-deposition coupling with a real-time poling approach. This new method has enabled the desired films to yield marked second harmonic generation characteristics even at relatively low poling fields, such as 0.01 MV/cm. Higher poling fields have also resulted in a stronger SHG signal. The uncured poly(amic acid) matrix may degrade due to moisture absorption, which in turn would result in the deterioration of the SHG signal. Curing the specimens at a moderately high temperature has greatly improved the film's integrity and likewise the NLO characteristics. A higher curing temperature is expected to yield a more thermally stable thin film, provided a more thermally stable NLO-active chromophore is available.

References and Notes

(1) Prasad, P. N.; Williams, D. J. *Introduction to Nonlinear Optical Effect in Molecules and Polymers*; Wiley: New York, 1991.

(2) Singer, K. D.; Sohn, J. E.; Lalama, S. J. *Appl. Phys. Lett.* **1986**, *49*, 248.

(3) Eich, M.; Reck, B.; Yoon, D. Y.; Willson, C. G.; Bjorklund, G. C. *J. Appl. Phys.* **1989**, *66*, 3241.

(4) Kajikawa, K.; Nagamori, H.; Takezoe, H.; Fukuda, A.; Ukishima, S.; Takajashi, Y.; Iijima, M.; Fukada, E. *Jpn. J. Appl. Phys.* **1991**, *30*, (10A), 1737.

(5) Yitzchaik, S.; Berkovic, G.; Krongauz, V. *J. Appl. Phys.* **1991**, *70*, 3949.

(6) Chen, M.; Daltan, L. R.; Yu, L. P.; Shi, Y. Q.; Steier, W. H. *Macromolecules* **1992**, *25*, 4032.

(7) Blanchard, P. M.; Mitchell, G. R. *Appl. Phys. Lett.* **1993**, *63*, 2038.

(8) Goodson, T., III; Gong, S. S.; Wang, C. H. *Macromolecules* **1994**, *27*, 4278.

(9) Yang, Y. R.; Ma, X. F.; Chen, W. X.; You, L.; Wu, P.; McDonald, J. F.; Lu, T.-M. *Appl. Phys. Lett.* **1994**, *64*, 533.

(10) Tsutsumi, N.; Fuji, I.; Ueda, Y.; Kiyotsukuri, T. *Macromolecules* **1995**, *28*, 950.

(11) Yu, D.; Gharavi, A.; Yu, L. P. *Appl. Phys. Lett.* **1995**, *66*, 1050.

(12) Veriest, T.; Burland, D. M.; Jurich, M. C.; Lee, V. Y.; Miller, R. D.; Volksen, W. *Science* **1995**, *268*, 1604.

(13) First, the NLO molecule is assumed to have a dipole moment, μ, mass, m, and charge group centers distance, $2a$. The moment of inertia of the molecule is assumed to be ma^2. The equation of motion for a polar molecule in a uniform poling field is

$$ma^2 \frac{d^2\theta}{dt^2} = \vec{\mu} \times \vec{E} = -\mu E \sin\theta$$

Accordingly, for an NLO molecule at an angle θ, the poling time, t_p, can be solved as[20]

$$t_p = \frac{\pi}{2}\sqrt{\frac{ma^2}{\mu E}}\Big\{1 + \Big(\frac{1}{2}\Big)^2 k^2 + \Big(\frac{1\times 3}{2\times 4}\Big)^2 k^4 + \Big(\frac{1\times 3\times 5}{2\times 4\times 6}\Big)^2 k^6 + ...\Big\}$$

In the present system, the DR-1 molecule has a molecular mass of 314 g/mol, dipole moment of 8.72 D[1], and $2a$ = 14.5 Å.

(14) Since eq 1 does not converge rapidly in such a case, the first 1000 terms of the series are summed up to obtain an approximated value, which is

$$2.86 \times \frac{\pi}{2}\sqrt{\frac{ma^2}{\mu E}}$$

This value is estimated to have an error of less than 1% from the precise one.

(15) In the poling zone, the traveling time of the NLO molecules is estimated by dividing the length of the poling zone with the velocity of the molecules. The poling length is assumed to be equal to the electrode thickness, which is 0.3 μm. The velocity of the molecule is assumed to be equal to 1.732 $\sqrt{kT/m}$, where K is the Boltzmann's constant and T the final temperature of the DR1 molecule before entering the poling zone. This temperature should be different from its evaporation temperature since collision with the other kinds of molecules would happen during the flight in the chamber. Therefore, T must be somewhere between the evaporation temperature and the temperature at equilibrium, which are 150 and 127 °C, respectively. The respective traveling times will be 1.63×10^{-9} and 1.67×10^{-9} s for these two different temperatures. No matter which extreme is taken into consideration, the traveling time is sufficiently long for the dye molecules to be poled into the desired orientation.

(16) Iijima, M.; Takahashi, Y. *Macromolecules* **1989**, *22*, 2944.

(17) Iijima, M.; Takahashi, Y.; Oishi, Y.; Kakimoto, M.; Imai, Y. *J. Polym. Sci.* **1991**, *A29*, 1717.

(18) Bellamy, L. J.; *The Infra-red Spectra of Complex Molecules*; Chapman and Hall: London, 1975; pp 331−339.

(19) Wu, J. W.; Binkley, E. S.; Kenny, J. T.; Lytel, R. *J. Appl. Phys.* **1991**, *69*, 7366.

(20) Spiegel, M. R. *Theory and Problems of Theoretical Mechanics*; McGraw-Hill Book Co.: London, 1980; p 105.